G-2

THE TIME DEPENDENT FRACTURE OF VISCOELASTIC MATERIALS*

W. G. Knauss+

ABSTRACT

Continuum mechanical aspects of the fracture process have been combined with microscopic considerations to evolve a simple model for the time dependent fracture process. According to this model, fracture occurs when a dominant defect develops to a size which is critical for the existing boundary loading.

Starting from the idea of spatial variations in the density of the molecules and their binding energy, an expression is developed for the rate of defect initiation. Under this concept flaws need not pre-exist in the material as discontinuities but may develop under sufficient loading from weak regions where molecular bonds are such that they do not possess their maximal strength.

In the absence of adequate information on the growth behavior of macroscopic cracks the defect initiation relation has been used as an approximation to the growth history of cracks. In conjunction with a critical crack size criterion of the Griffith type, suitably modified by Rivlin and Thomas to account for viscoelastic solids is shown to correlate well with experimental data.

While the complexity of the fracture problem in viscoelastic solids dictates a number of assumptions in any analytical approach, the relatively close corroboration of the ideas presented in this paper with experimental evidence speaks for the fundamental role they play in viscoelastic fracture.

+ Assistant Professor of Aeronautics, California Institute of Technology, Pasadena, California

* Part of this work is based on a Ph.D. Dissertation submitted to the California Institute of Technology, June 1963, which was supported by the National Aeronautics and Space Administration, Research Grant No. NsG-172-60.

INTRODUCTION

In the past few years increased dependence of engineering design on polymeric materials has called for a proportional understanding of ultimate behavior of such solids. While a considerable amount of experimental data has accumulated, there remains a great number of fundamental questions which need to be answered before a reasonably satisfactory theory of fracture in viscoelastic materials can be developed. For example, very little is known quantitatively about the fracture initiation process on the molecular level; similarly, on a macroscopic scale, the laws governing the viscoelastic behavior of materials undergoing large deformations have not yet been formulated quantitatively in a practical manner, so that a precise large-deformation viscoelastic stress analysis for even relatively simple test geometries is not yet possible. In view of these most obvious difficulties any theory offered at this time and irrespective of its apparent successes should be regarded as an exploration of certain concepts rather than as a definitive statement.

Several theories of fracture in polymers have been advanced [1, 2, 3, 4, 5]. Their common limitation seems to be an oversimplified view of the fracture process, and, particularly, an inadequate description of the continuum mechanical aspects of gross rupture. While these simplifications lead also to uncomplicated mathematical expressions the resulting calculations are applicable only over limited ranges of time and temperature. A notable exception is the theory of Bueche and Halpin[4] which was developed concurrently with the theory presented here[6]. These authors based their calculation on the experimental findings of Smith[7,8] to which we shall refer in detail later, and on a concept of crack propagation advanced by Williams[9,10]. While the resulting calculations corroborate the experimental findings of Smith reasonably well the physical phenomena offered in explanation of the calculations hardly withstand a critical examination. A further limitation of the theory is its orientation toward failure in uniaxial stress states and the lack of provision to extend it to failure in multiaxial stress states. Although we shall demonstrate the calculations for the theory presented in this paper on failure in essentially uniaxial stress states the present work is equally applicable to failure in multiaxial stress states.

The experimental work of Smith from which Bueche and Halpin developed their theory has also been restricted to uniaxial tensile tests. In an effort to arrive at a more precise description of the failure properties by reducing the scatter of failure data obtained in uniaxial, constant strain rate tests, Smith plotted the stress at break against the strain at break and called the resulting curve a failure envelope. He then noted that the failure data obtained in constant load and constant strain tests coincided with the failure envelope derived from failure tests under constant strain and constant load to rupture. He therefore suggested that the failure envelope determines the failure properties for arbitrary load histories. Inasmuch as viscoelastic materials are distinguished from others by the fact that their stress-strain response

depends on the history of deformation, it appears surprising that the accumulation of failure should be independent of the infinite number of load histories which could lead to the same stress-strain state. We shall see later that the three load histories employed by Smith are of a very similar nature and that different types of loading histories could lead to fracture behavior not predicted by the failure envelope.

THE FAILURE MODEL

Failure in polymeric materials may occur either by excessive permanent flow deformation or by fracture. While crosslinked polymers fail only by fracture, linear polymers may fail both by flow and fracture depending upon the rate of load application and the temperature. In this work we shall be concerned only with the fracture of polymers. Since fracture is the result of crack growth we shall first derive from experimental studies some ideas on the propagation of cracks.

In our later work we shall be concerned with three particular facets of crack growth, namely:

1) the energy required to propagate a crack;

2) the relation of fracture surface markings to propagation speed;

3) the growth rate behavior of relatively small cracks;

these we consider now briefly in turn.

When a new surface of unit area is formed in a solid a certain amount of energy is required[11,12,13]. This fracture energy is equal to the work required to rupture inter-atomic bonds of the molecular structure (surface energy) and other dissipative losses at the tip of an advancing crack[10,14]. Because of their rate sensitive properties viscoelastic materials possess fracture energies which depend strongly on the rate of crack propagation[15,16].

An example of this velocity dependence is given by the energy required to propagate a crack at a constant rate through a thin sheet. If a long strip containing a crack along its major dimension (cf. Figure 1A) is clamped at the long edges and strained uniformly across the width, then the crack will propagate at a constant rate, provided the strain is sufficiently high and the polymer is in its long-time, rubbery state. If, furthermore, no work is done on the sheet during crack propagation then the fracture energy T is equal to the energy stored elastically per unit strip length in the uniformly strained region ahead of the crack[13,14]. One may thus determine the fracture energy from the stress-strain behavior of the strip geometry without a crack and the applied strain and relate it to the measured crack propagation velocity. As an example, Figure 2 shows the fracture energy T as a function of the crack propagation speed for an H-C rubber* used extensively in this work.

* The author is indebted to Drs. R. B. Kruse and T. A. Neely of the Thiokol Chemical Corporation for supplying the material for these studies.

In the same figure the velocity range has been divided into three parts according to the appearance of the fracture surface. For crack speeds below approximately 10^{-2} inches per minute the fracture surface of the H-C rubber is rough; crack propagation appears to take place through the formation of polymer ligaments (cf. Figure 3) which then rupture and thus effectively advance the crack tip. At higher speeds, there is insufficient time to permit extensive ligament formation and the fracture surface becomes progressively smoother as the velocity increases. This is evident in Figure 4 which shows fracture surfaces resulting from steady state crack propagation tests as described above.

The same transition from rough to smooth fracture surface is observed for cracks which propagate non-steadily such as in fracturing tensile specimens. With information of the type embodied in Figure 4 one is thus able to obtain a qualitative picture of the rate of crack growth during the fracture process. Figure 4 shows a series of fracture surfaces on tensile specimens failed under various strain rates and stress levels. The change from slow to fast crack growth is clearly evident. However, note also that with increasing strain rate, which implies increasing fracture stress, the rough area formed by slow crack growth diminishes. An equivalent statement of this observation is that the critical crack size at which transition from slow to fast crack propagation occurs decreases with increasing failure stress level. For the reader who is familiar with the calculations derived by Griffith[11] for brittle materials this inverse relation between failure stress and critical crack size is referred to a crack velocity transition instead of velocity initiation. We shall use this fact later to establish a rupture criterion for viscoelastic materials.

It remains now to examine the relative time spans of the initial slow and the final fast rate of crack growth in a tensile specimen. It is conceivable that the final stage of fast crack growth is insignificantly short when compared to the time required to develop a crack to the size at which transition from slow to fast growth takes place. In this case fracture could be characterized in terms of the slow-to-fast crack speed transition and a detailed treatment of the final rupture stages would play an insignificant role in fracture prediction. That this seems indeed to be a reasonable assumption is evident from Figure 6 which shows growth histories of identical cuts in strip specimens as shown in Figure 1B. While the period of slow crack propagation could have been prolonged considerably by making the initial cuts smaller, it is obvious from this data that the time of slow crack propagation tends to be long compared to the final stage of crack growth.

Although one expects that materials which are different from the H-C rubber employed in these tests yield quantitatively different results, the same qualitative behavior should be observed. We proceed therefore to incorporate these past experimental observations into a fracture criterion.

In order to calculate the time of fracture we envisage the following model of the rupture process. A crack may develop from a

microscopic or macroscopic defect and grows relatively slowly until it reaches a critical size, after which instant it propagates fast until complete rupture of the specimen occurs. The time of fracture is given essentially by the time required for slow crack propagation, and it is determined by a suitable criterion of critical crack size. We proceed now first to establish such a criterion after which we consider the initiation and slow growth stage of a crack.

A Condition of Critical Crack Size. As an introduction let us recall briefly the ideas which lead to the prediction of fracture in brittle materials containing cracks. The basic concept underlying the calculations by Griffith[11] is the law of conservation of energy, or more explicitly the transformation of elastically stored energy into surface energy as a crack increases by an infinitesimal amount. Mathematically the condition that one or several cracks in a stressed body become unstable is given by the condition

$$\dot{F} + \dot{D} - \dot{W}_B \leq 0 \tag{1}$$

where $\dot{F}$ = rate of change of free energy

$\dot{D}$ = rate of energy dissipation

$\dot{W}_B$ = rate of work of the boundary forces.

Noting that for brittle materials the energy dissipation per unit of new crack area is equal to the surface energy γ one has

$$\dot{F} - \dot{W}_B \leq - \gamma \frac{dA}{dt} \tag{2}$$

where A is the area of the crack. For the case of a centrally cracked plate of unit thickness under a uniform peripheral stress σ, Griffith showed that the inequality predicts catastrophic failure when

$$\frac{\pi}{2} \frac{\sigma^2}{E} c \geq \gamma \tag{3}$$

with c as the half crack length.

The derivation of an equivalent relation for the prediction of fracture in viscoelastic materials meets two major difficulties, namely that 1) the shape of the cracks is in general not known and 2) the necessary stress analysis is intractable when large strains are encountered*. Although a detailed qualitative analysis involving various arguments on the above two points can lead to the result below, its derivation rests ultimately on arguments of dimensional analysis. In the interest of brevity and clarity we present therefore on dimensional grounds the analog to relation (3) for a viscoelastic solid as

$$W_{el} c_{crit} \geq \kappa T (\dot{c}_{crit}) \tag{4}$$

where c_{crit} = expresses the size of the crack just prior to

* An exception is the analysis of fracture initiation from a spherical void in a uniform hydrostatic tensile stress field. (Ref. 15).

rapid crack growth

W_{el} = the elastically stored energy density far away from the crack

κ = a proportionality constant

T = fracture energy commensurate with the rate of crack growth $\dot{c}_{crit}$.

The prediction of failure is thus based on the relatively simple condition that the product of the free energy W_{el} and the crack size c, both of which depend on the strain history of the material, reaches a critical value at failure. Furthermore, the constant κ should be approximately equal to $2/\pi$ and the value for T for the H-C rubber should be on the order of 0.5 pounds per inch according to Figure 2.

Crack Initiation. It is common in failure analyses to assume that fracture starts from surface cracks which were introduced in the process of specimen preparation. While this is probably true in many instances, it is also observed that fracture starts in the interior of a specimen[16,17]. It is therefore appropriate to consider the more general situation in which fracture can start at an arbitrary point in the material. Later, such points of fracture initiation may be easily interpreted as surface defects.

We have already mentioned in the introduction that the molecular processes involved in the initiation of fracture are poorly understood. While the nature of fracture initiation can hardly be determined without extensive and purposeful experimentation, it is nevertheless interesting to speculate as to possible mechanisms which may take part in the fracture process.

Although many polymeric solids seem to be isotropic and homogeneous continua, this appearance breaks down when they are examined on a microscopic scale. At this level of observation one would encounter spatial variations in the densities of molecules, chain entanglements and in crosslinks as well as bond strengths. Such variations in the molecular structure are likely sites of failure initiation. For instance, a locally low crosslink density might facilitate local slippage of molecule chains and thus contribute to the formation of a small void. Such a mechanism may account for the low strength values found by Sookne and Harris[18] for polymer blends involving small amounts of low molecular weight material. Similar effects may be expected from regions of low molecular density or low molecular bond strength.

In the absence of a more precise description of the initial flaw character, we may thus imagine a polymeric structure of preferred strength regions interspersed with weak regions where molecular configurations would favor rupture initiation. In order to arrive at a quantitative evaluation of the defect growth within a weak region, we make the following assumptions:

1) Defect growth is due to bond rupture and chain slippage. Successive bond rupture depends on chain slippage, and vice versa.

2) Bond rupture or chain slippage occurs spatially at random within a weak region; newly created radicals do not affect unbroken bonds.

3) Bonds may reform and new chain entanglements may develop. The resulting configurations are indistinguishable from the original ones.

4) Each weak region contains a large but finite number of breakable bonds.

Under these conditions it is possible to derive an expression for the net increase of broken bonds by using linear rate law theory[19,20]. Let N_1 and N_2 denote, respectively, the number of unbroken and broken bonds. The increase of broken bonds N_2-N_1 is then given by the differential equation

$$\frac{d}{dt}\left\{\frac{N_2-N_1}{N_o}\right\} = -(\overline{\omega_{12}}+\overline{\omega_{21}})\left\{\frac{N_2-N_1}{N_o}\right\} + (\overline{\omega_{12}}-\overline{\omega_{21}}) \qquad (5)$$

where $N_o = N_1 + N_2$ = constant

$\overline{\omega_{12}}$ = rate constant determining the average rate of bond rupture

$\overline{\omega_{21}}$ = rate constant determining the average rate of bond formation.

For our purposes, it suffices to consider only the particular solution of the differential equation (5)*. If one assumes that the number of broken bonds in a weak region is proportional to the effective area of a defect, one finds the time dependent area of the defect by integration of (5) as

$$\frac{A}{A_o} = \exp\left\{-\int_o^t(\overline{\omega_{12}}+\overline{\omega_{21}})dt\right\}\int_o^t\left\{(\overline{\omega_{12}}-\overline{\omega_{21}})\exp\left[\int_o^\tau(\overline{\omega_{21}}+\overline{\omega_{12}})d\theta\right]\right\}d\tau \qquad (6)$$

where A_o is a normalizing constant area.

In order to obtain the rate functions $\overline{\omega_{12}}$ and $\overline{\omega_{21}}$ consider a large number of identical polymer chain links under equal loads. If an amount of energy h is required to break a single bond then the theory of rate processes[20] predicts, for example, that

* The number of broken bonds in the equilibrium state (zero stress) depends upon the relative magnitude of the rate functions $\overline{\omega_{12}}$ and $\overline{\omega_{21}}$ at equilibrium which are then more appropriately called equilibrium constants. Although the equilibrium constants must be determined by experiment it is more convenient to choose them equal in magnitude. This implies (cf. Eqn. 5) that the number of broken bonds is equal to the number of unbroken bonds in the equilibrium state. Inasmuch as we are interested only in a deviation from the reference state this assumption is not very critical; the general character of the solution is not changed.

$$\omega_{12} = \frac{kT}{\hbar} e^{-\frac{h-f}{kT}} \tag{7}$$

where k = Boltzmann's constant

$\hbar$ = Planck's constant

T = absolute temperature and

f = elastic energy per bond.

If there exists a distribution of bond strengths $\varphi(h)$ rather than a single value the average rate functions can be expressed approximately as[6,19]

$$\overline{\omega_{12}} \doteq \frac{\lambda}{2} \Theta(T)\, e^{\frac{f}{kT}}$$

$$\overline{\omega_{21}} \doteq \frac{\lambda}{2} \Theta(T)\, e^{-\frac{f}{kT}} \tag{8}$$

where λ is a constant and $\Theta(T) = \int_0^\infty \varphi(h)\, e^{-\frac{h}{kT}} dh$ is a function of the temperature only.

Equations (5) and (6) become thus, respectively,

$$\frac{dA/A_o}{dt'} = -\lambda \left\{ \frac{A}{A_o} \cosh \frac{f}{kT} - \sinh \frac{f}{kT} \right\} \tag{9}$$

and

$$\frac{A}{A_o} = \exp\left\{ -\lambda \int_o^t \cosh \frac{f}{kT} dt' \right\} - \int_o^t \lambda \left\{ \sinh \frac{f}{kT} \left[\exp \lambda \int_o^\tau \cosh \frac{f}{kT} d\theta \right] \right\} d\tau' \tag{10}$$

where we have written dt' for $\Theta(T)dt$. The prime notation signifies the usual temperature reduced time for thermorheologically simple materials. Either of equations (9) or (10) determine the size of a defect as a function of the loading history through the rate dependent elastic energy f.

The elastic energy f per bond may be obtained approximately from the phenomenological stress-strain law for any desired loading history and by then dividing the elastic strain energy density by the number N of breakable bonds within a weak region, i.e., $f = W_{el}/N$. Of course, we consider here only the elastic or free energy because the energy dissipated in deformation processes contributes merely to raising the temperature while only the free energy contributes directly to the fracture process[3].

Crack Growth. Having considered the crack initiation stage from a quasi-molecular viewpoint we need to be concerned now with the growth of such defects into cracks which become sufficiently large to cause failure. The laws which govern this growth stage are poorly, if at all, understood[4,9,10]. We therefore propose to use the

previously derived defect initiation relation (10) as an approximate description of the time dependent growth of a crack until it reaches a size which is critical in terms of the energy balance equation (4).

While such an approximation is not completely arbitrary, it is also gratifying to note that it may be physically not unreasonable, although the molecular mechanisms implied by equation (10) are probably not quite the same as those responsible for crack growth outside of the postulated weak regions.

The reason that the approximation may be a reasonable one can be found in a qualitative comparison with the experimental work of Regel[21], who measured the growth of cracks in plasticized polymethylmethacrylate under a constant applied stress. Since for his experiments the elastic energy did not change appreciably with time, equation (10) would predict a time dependent length of surface cracks with approximately constant depth as

$$\frac{\ell}{\ell_o} = \tanh \frac{W_{el}}{NkT} \left\{ 1 - \exp\left[-\lambda t \cosh \frac{W_{el}}{NkT} \right] \right\} \tag{11}$$

Figure 7 shows a qualitative comparison of equation (11) with Regel's data. The similarity of the theoretical expression and the measurements is evident. It should be repeated, however, that the differential failure equation (9) is, at this time, an expedient assumption. Its special value rests in the fact that it agrees well with both direct and indirect measurements and that it accommodates arbitrary loading histories.

It may be noted in passing that there exists a similarity between equation (10) on the one hand and the strain in a linearly viscoelastic material subjected to an arbitrary stress history on the other. If one defines the function

$$F(t,\tau) \equiv \exp\left\{ -\lambda \int_\tau^t \cosh \frac{W_{el}}{NfT} d\tau \right\} \tag{12}$$

then equation (10) may be written as a non-linear superposition integral

$$\frac{A(t)}{A_o} = \lambda \int_o^t F(t,\tau) \sinh \frac{W_{el}}{NfT} d\tau \tag{13}$$

while the uniaxial strain for a linearly viscoelastic material is given by the linear superposition integral

$$\epsilon(t) = \int_o^t D(t,\tau) \frac{d\sigma}{d\tau} d\tau \tag{14}$$

where $D(t)$ is the strain-independent creep compliance and σ is the stress.

In principle, we have now completed the prediction of fracture within the framework of our simplified fracture model. By using equation (13) to calculate the time dependent crack size we may determine from the criticality condition (4) the time when this crack progresses into the final fracture stage. In the next section we consider now the application of the equations (4) and (13) to some practical test situations.

APPLICATION OF RUPTURE PREDICTION

The calculation of the fracture properties from the crack growth relation (13) and the critical crack size condition (4) requires knowledge of the free energy density. As was pointed out in the introduction, the mathematical formulation of large deformation viscoelasticity is in an embryonic stage and the determination of such an uncommon function as the free energy appears difficult at best. We shall therefore replace the non-linear stress-strain law by a modified linear one such that the energy density as calculation from the two stress-strain relations agree reasonably well.

It has been found[22, 23, 24, 25] that the stress in a large deformation relaxation experiment is given by the time-strain factorized form

$$\sigma(\epsilon, t) = E_{rel}(t)\, f(\epsilon) \tag{14}$$

where $E_{rel}(t)$ is the relaxation modulus for small strains (cf. Figure 8A) and $f(\epsilon)$ is a nonlinear function of the strain ϵ which reduces to ϵ for small strains. When viscoelastic processes are absent one has also

$$\sigma = \sigma(\epsilon) = E_R\, f(\epsilon) \tag{15}$$

where now E_R is the long time or rubbery modulus. This relation is shown in Figure 9A for H-C rubber. Shown in the same figure is a linear approximation

$$\sigma = \alpha E_R\, \epsilon \tag{16}$$

where α is an appropriately chosen constant. It turned out that a suitable choice is $\alpha = 0.22$ for the material used. Because the energy is obtained from the stress-strain relation by integration its functional dependence on the strain is very similar for the two stress-strain laws as shown in Figure 9B. Henceforth, we approximate the energy density in a solid undergoing large deformations by the energy density in a linear solid, the modulus of which is a fraction of the small strain modulus of the nonlinear solid, even when viscoelastic effects are present.

Turning now to the calculation of the elastic energy in a linearly viscoelastic solid, recall that the mechanical properties may be represented by mechanical spring and dashpot models[25, 27, 28]. For instance, the generalized Maxwell or Wiechert model in Figure 10A may be used to represent the relaxation modulus for the H-C rubber shown in Figure 10A if 17 spring-dashpot combinations are

used. The relaxation modulus is then represented by

$$E_{rel}(t) = m_e + \sum_{i=1}^{17} m_i e^{-t/\tau_i} \tag{17}$$

provided $\tau_i = 10^{-(i+1)}$. The elastically stored energy is then the energy stored in the spring elements of the model. Similarly, the energy dissipated during deformation of the viscoelastic solid is represented by the work done in extending the dashpot elements. In order to correct for the nonlinear nature of the stress-strain behavior we multiply the individual spring constants by the correction factor α.

The Constant Strain-Rate Test. The experimental determination of the ultimate uniaxial tensile data for the H-C rubber employed in this work is given in detail elsewhere[29] and need not be repeated here.

As the strain $\epsilon(t) = R \cdot t$, prescribed to increase linearly with time, is the same for all the elements in the Wiechert model (springs and dashpots in series) one finds for the stress in the ith spring and dashpot

$$\sigma_i = m_i \tau_i R \left(1 - e^{-t/\tau_i}\right) \tag{18}$$

where $\tau_i = \eta_i / m_i$ is the relaxation time of the ith Maxwell element. The energy in the ith spring is therefore

$$W_i = \frac{\sigma_i^2}{2m_i} = \frac{1}{2} m_i (\tau_i R)^2 \left\{1 - e^{-t/\tau_i}\right\}^2 . \tag{19}$$

The total elastic energy is thus given by

$$W_{el} = \frac{\alpha}{2} m_e (Rt)^2 + \frac{\alpha}{2} \sum_{i=1}^{17} m_i (\tau_i R)^2 \left\{1 - e^{-t/\tau_i}\right\}^2 \tag{20}$$

where the first term represents the energy in the degenerate Maxwell element and α is the empirical correction factor to account for the non-linear material behavior.

Using expression (20) we can now calculate the crack size by numerically integrating the differential failure equation (9). Since failure usually starts from the corner (cf. Figure 5) and extends over a triangular region the crack area is proportional to c^2, c being the crack dimension along the surface of the specimen. When this dimension reaches the critical value prescribed by the condition (4) the specimen has failed. The result of these calculations are shown in Figure 11 together with the experimental data.

The Dual Strain-Rate Test. In order to demonstrate in more detail the effect of the strain rate history on the failure properties we consider now a uniaxial test which involves two constant strain rates

instead of the previous single one. This strain history may be considered as a simple model of a more general variable strain rate history. Figure 12 shows a set of dual strain rate histories for two arbitrarily selected strain rate values and the corresponding calculated rupture points for the same material represented in Figure 11. Since the calculations for this type of strain rate history are essentially the same as for the constant strain rate test they need not be outlined specifically.

Harstad has verified these calculations qualitatively on an H-C rubber of slightly different formulation than that represented by Figures 8 and 11. His results are shown in Figure 13[30]. Although the data scatter is considerable it is nevertheless clear that the order in which high or low strain rates are applied has a significant effect upon the ultimate properties. This result is similar to that which Valluri found for metal fatigue[31].

Crack Propagation at Constant Velocity. As a further example of a different type of rupture experiment we consider the steady propagation of a crack through the strip geometry shown in Figure 1A. Although the previous rupture calculations considered the growth of a crack in a macroscopic tensile sample similar to the crack in the stressed sheet, it should be interesting to apply these calculations to the fracture of small material filaments (9) undergoing tensile rupture at the tip of a crack.

In terms of the present failure model we envisage the process of crack propagation to occur in the following manner: As a point on the line of crack propagation is approached by the steadily advancing crack tip it experiences a time dependent strain rate arising from the stress concentration at the crack tip; accordingly microscopic defect growth occurs at that point with a rate determined by the differential failure equation (9). But when the point is just reached by the crack tip the combination of local defect size and elastic energy must satisfy the critical condition (4).

For reasons of mathematical simplicity we limit the occurrence of rupture to a narrow band along the line of crack propagation across which the stress conditions are essentially uniform. Neglecting inertia effects for slowly moving cracks* one can deduce from the stress analysis for this geometry[19,32] that the stress across the narrow band, σ_y, is approximately equal to

$$\sigma_y = \sigma_\infty \left\{ \frac{0.5\sqrt{b}}{\sqrt{x+\rho}} + 1 - \frac{1}{2}\left[e^{-\frac{x}{3b}} + e^{-\frac{5x}{2b}} \right] \right\} \qquad (21)$$

* Based on the equilibrium shear modulus of the H-C rubber studied here the equivoluminal wave speed is 10^5 in/min ($\sim$150 ft/sec). Speeds below 10^3 in/min should therefore be admissible for this analysis; the maximum velocity measured in the experimental studies was approximately 100 in/min.

where x is the distance from the crack tip, b is the half width of the test strip and ρ has the meaning of a crack tip radius. A complication arises from the presence of the σ_x stress parallel to the direction of crack propagation. In order to keep the calculations simple we will neglect this stress* and reduce the problem of crack propagation to a problem in uniaxial tensile failure under a special stress history.

Making the steady state velocity transformation $\xi = x - vt$ where v is the (unknown) crack velocity we consider therefore a small uniaxial tensile specimen as located at $x = x_o$ far ahead of the crack and subject it to the stress history

$$\frac{\sigma}{\sigma_\infty} = \frac{\sigma(t)}{\sigma_\infty} = \frac{0.5\sqrt{b}}{\sqrt{\xi+\rho}} + 1 - \frac{1}{2}\left\{ e^{-\frac{\xi}{3b}} + e^{-\frac{5\xi}{3b}} \right\} \qquad (22)$$

with $\xi = x_o - vt$. The problem of crack speed determination consists thus of finding the value of the velocity for a given value of the applied stress σ_∞ such that the criticality equation (4) is satisfied when $\xi = 0$.

The time dependent elastic energy at a point undergoing eventual rupture can be calculated again with the help of a viscoelastic material model by summing the energy stored in the springs of the model. But because the stress is now prescribed we employ the generalized Voigt model in Figure 10B. The strain in the ith Voigt element is determined from Duhamel's Integral as

$$\epsilon_i(t) = \int_o^t \frac{\sigma(t-\theta)}{m_i \tau_i} e^{-\theta/\tau_i} \, d\theta \qquad (23)$$

and upon using the stress (22) there results

$$\epsilon_i(t) = \frac{\sigma_\infty}{m_i \tau_i} \left\{ \frac{0.5\sqrt{b}}{\sqrt{v\tau_i}} e^{\frac{\xi+\rho}{v\tau_i}} \Gamma\left(\frac{1}{2}, \frac{\xi+\rho}{v\tau_i}\right) + 1 - \frac{b}{2}\left[\frac{3e^{\frac{\xi}{3b}}}{v\tau_i+3b} + \frac{2e^{-\frac{5\xi}{2b}}}{5v\tau_i+2b} \right] \right\} \qquad (24)$$

where $\Gamma(\frac{1}{2}, u)$ is the incomplete gamma function of order 1/2. By summation of the energy in the springs of the generalized Voigt model the total time dependent energy is obtained as

* Although the σ_x stress is by definition zero at the crack boundary it is not zero ahead of the crack where its value is a fraction of the σ_y stress. (It is also a tensile stress.) Note, however, that as the shear stress is zero on the crack axis the energy density there is, for an incompressible solid,

$$W_{el} = 1/2m_e\left[\sigma_y^2 + \sigma_x^2 - \sigma_x\sigma_y\right];$$

this has a minimum for $\sigma_x = \sigma_y/2$ which is, however, only 25 percent smaller than when $\sigma_x = 0$. Neglecting the σ_x stress should therefore not influence the results any more seriously than the unknown crack tip radius ρ.

$$W_{el} = \frac{1}{2}\frac{\sigma_y(t)^2}{m_g} + \frac{1}{2}\sum_{i=1}^{17} m_i \epsilon_i^2 \qquad (25)$$

with m_g representing the short time response modulus of the material. The use of the energy relation (25) permits again the numerical integration of the defect rate equation (9).

Greensmith[33,34] has related the effective radius of curvature to the roughness of the fracture surface. According to the earlier discussion on the appearance of the fracture surface the roughness and thus the tip radius decreases with increasing crack speed. It turns out however, that a velocity dependent radius of curvature does not lead to a significantly different result, so that a constant radius was used in the calculations. A particular value of $\rho = 0.01$ inches was chosen to make the theoretical results coincident with experiment.

Since the radius of curvature is an unknown parameter in these calculations the computation of crack velocities actually amounts to a determination of this quantity. The value of $\rho = 0.01$ inches is consistent with the findings of Greensmith[34] who measured effective radii between 0.01 and 0.02 inches. The calculated velocity values are shown as the solid curve in Figure 14 together with the experimental data.

EVALUATION OF THE FAILURE MODEL

Until now we have withheld discussion of the past calculations in order to present it from a unified viewpoint. Due to the proper choice of the unknown parameters the agreement between theory and experiment is quite satisfactory considering the fact that a linear stress-strain law was used in place of a nonlinear one. Indeed, all the discrepancies are consistent with the approximation of the stress-strain law.

We have already mentioned that of the several constants entering the failure equations (4) and (9), the fracture energy T and the crack geometry constant κ should have the approximate values of 0.5 pounds per inch and $2/\pi$, respectively. Furthermore, it turned out that the normalizing area A_o in the differential failure equation (9) could be taken equal to the cross-sectional area of the tensile specimens. In the case of the crack propagation calculations this value is of questionable meaning. While, in principle, the constant N in equation (9) should be derivable from molecular considerations, it was here simply chosen to make the calculations agree best with the experimental data. The same is true for the constant λ, for which there does not seem to be an a priori estimate. It turned out, however, that the calculations were not very sensitive to its value and it was thus chosen as unity (minute^{-1}).

Using these constants permitted also the calculation of the critical crack size at failure. For the constant strain rate tests this crack size is shown as a function of strain rate in Figure 15. The values are quite commensurate with the experimentally observed ones (see, for instance, Figure 5).

Finally, we turn to the consideration of the failure envelope concept proposed by Smith[8]. In this form of failure data presentation, the discrepancy between the experimental data and the theory based on the linearly viscoelastic theory is most obvious at low stress levels. This may be seen in Figure 16 where the dashed curve represents the calculations based on the linear stress-strain law and the solid line has been corrected for non-linear effects in accordance with Figure 9A.

Recall from the introduction that it has been suggested on the basis of constant load, constant strain and constant strain rate tests, that the failure envelope predicts failure for arbitrary strain rate histories. The reason that these loading histories lead to equal rupture stresses and strains may be due to the fact that they do not give rise to markedly different stress histories near the rupture point. Inasmuch as it has been demonstrated previously that failure accumulation is stronger the closer the failure point is approached[19] one should perhaps not expect too much variation in failure behavior under these loading histories. Note also, that the strain histories of these tests are such that $d^2\epsilon/dt^2 \leq 0$ for all of them. Figures 17A and B show a series of loading histories and the corresponding stress-strain traces. Only those stress-strain curves for which $d^2\epsilon/dt^2 > 0$ deviate markedly from the other ones near the failure point.

Following these observations, the calculated failure behavior in the dual strain rate tests was entered on the failure envelope plot. The failure behavior in the fast-slow sequence, shown as the heavy black circles in Figure 16, was virtually indistinguishable from the constant strain rate rupture behavior. In contrast, the slow-fast strain rate sequence gave rise to the trace determined by the heavy black triangles, which distinctly do not fall on the envelope. While the difference of failure under the two strain histories is not large for the relatively small range in strain rates considered in these hypothetical tests, and while this difference could be masked by the usual data scatter, it is possible that a wider range of dual strain rates results in a larger discrepancy with the failure envelope.

In terms of the present failure theory this effect of load history upon the stress and strain at failure can be explained simply. Recall from the initial discussion on the criticality of crack sizes that at low stress levels a crack will grow to a larger size before onset of rapid crack propagation than it would at a comparatively higher stress level (see also Figure 5). It follows that a crack size which has developed in a low stress field to a size which is subcritical for that stress level may suddenly become critical, even without further growth, if the stress is raised by increasing the strain rate. For such a strain history one has the condition $d^2\epsilon/dt^2 > 0$. On the other hand, if $d^2\epsilon/dt^2 \leq 0$, then the defect will always be subcritical for successive

stress states until fracture occurs.* On the basis of this admittedly limited exploration of loading history effects, one might expect that the failure envelope characterizes failure behavior within experimental accuracy whenever $d^2\epsilon/dt^2 < 0$. On the other hand, if $d^2\epsilon/dt^2 > 0$ such as may be the case when a viscoelastic material is subjected to low loads for extended periods of time and subjected intermittently and briefly to high stresses, then the failure envelope may provide a non-conservative means of predicting failure.

CONCLUSION

We have presented a theory of time dependent fracture which explicitly considers the accumulation of failure in terms of crack growth. Because precise analysis methods have not yet been developed for many of the problems involved in fracture, the theory is, perforce, approximate. Nevertheless, the relatively good agreement of the theory with practical laboratory experiments indicates that the major factors controlling the fracture process have been incorporated in the fracture model. Furthermore, the physical parameters which enter the calculations are of reasonable, practically observed, magnitudes.

Besides the good agreement with experiments this internal consistency of the theory seems to speak for the usefulness of the basic concepts which have been presented here.

* Strictly speaking the criterion for making a crack critical is not whether $d\epsilon^2/dt^2$ is larger or smaller than zero. This boundary is given more accurately by that strain rate history which produces a constant rate of crack growth. It is interesting to note in passing that this limit case has been artificially enforced in the theory of Bueche and Halpin[4] and therefore that theory may not lead to a universal description of fracture in arbitrary loading histories.

REFERENCES

1. Tobolsky, A. V., Eyring, H, J. Chem. Phys., Vol. 11, (1943), pp. 125-134.
2. Bueche, F., J. Appl. Phys., Vol. 26, (1955), pp. 1133-1140.
3. Bueche, F., J. Appl. Phys., Vol. 28, (1957), pp. 784-787.
4. Bueche, F., Halpin, J.C., Technical Documentary Report No. ASD-TDR-63-483, Wright-Patterson Air Force Base, Ohio, August 1963.

   See also: Halpin, J.C., J. of Appl. Phys., Vol. 35, No. 11, November 1964, pp. 3133-3141.

   and, Halpin, J. C., Bueche, F., J. of Appl. Phys., Vol. 35, No. 11, November 1964, pp. 3142-3149.
5. Zak, A. R., ARL 64-144, Office of Aerospace Research, United States Air Force, September 1964.
6. Knauss, W. G., GALCIT SM 62-28, California Institute of Technology, July 1962.
7. Smith, T. L., J. of Pol. Sci., Part A, Vol. 1, (1963), pp. 3597-3615.
8. Smith, T. L., J. of Appl. Phys., Vol. 35, No. 1, January 1964, pp. 27-36.
9. Williams, M. L., Blatz, P. J., Schapery, R. A., GALCIT SM 61-5, California Institute of Technology, February 1961. (ASTIA No. AD 256-905).
10. Williams, M. L., Fracture of Solids, Edited by D. C. Drucker and J. J. Gilman, John Wiley and Sons, (1963).
11. Griffith, A. A., Phil. Trans. Roy. Soc. (London), Series A, Vol. 221, (1920), pp. 163-198.
12. Irwin, G. R., Handbuch der Physik, Vol. VI, Springer, (1958).
13. Rivlin, R. S., Thomas, A. G., J. Pol. Sci., Vol. 10, (1952), pp. 291-318.
14. Thomas, A. G., J. Appl. Pol. Sci., Vol. 3, (1960), pp. 168-174.
15. Williams, M. L., Schapery, R. A., International Journal of Fracture Mechanics, Vol. 1, No 1, March 1965, pp. 64-72.
16. Bueche, A. M., White, A. V., J. Appl. Phys., Vol. 27, No. 9, September 1956, pp. 980-983.

17. Lindsey, G. H., Ph.D. Dissertation, 1966, California Institute of Technology, Pasadena, California.

18. Sookne, A. M., Harris, M., (1) Textile Research, Vol. 8, (1943), pp. 17-31. (2) Ind. Engr. Chem., Vol. 37, (1945), pp. 478-482.

19. Knauss, W. G., Ph.D. Dissertation, 1963, California Institute of Technology, Pasadena, California.

20. Glasstone, S., Laidler, K. J., Eyring, H., The Theory of Rate Processes. McGraw-Hill, New York, (1941).

21. Regel, V. R., Soviet Physics (Technical Physics), Vol. 1, No. 2, pp. 353-361, 1956-57.

22. Guth, E., Wack, P. E., Anthony, R. L., J. of Appl. Phys., Vol. 17,(1946), p. 347.

23. Landel, R. F., Stedry, P. J., J. Appl. Phys., Vol. 31, (1960), pp. 1885-1891.

24. Becker, G. W., Rademacher, H. J., J. Pol. Sci., Vol. 58, (1962), pp. 621-631.

25. Smith, T. L., Symposium on Stress-Strain-Time-Temperature Relationships in Materials. Published by the American Society for Testing and Materials, (1962), pp. 60-89.

26. Biot, M. A., Proceedings of the Third National Congress of Appl. Mech. (1958), pp. 1-18.

27. Biot, M. A., Phys. Rev. (1955), 97, pp. 1463-69.

28. Schapery, R. A., Ph.D. Dissertation, 1962, California Institute of Technology. Also, ARL 62-418, Office of Aerospace Research, United States Air Force, August 1962.

29. Knauss, W. G., GALCIT SM 63-1, California Institute of Technology, January 1963.

30. Harstad, K., GALCIT CP 63-2, California Institute of Technology, May 1963.

31. Valluri, S. R., Aerospace Engineering, Vol. 20, (1961), p. 18.

32. Knauss, W. G., GALCIT SM 65-1, California Institute of Technology, February 1965. To be published in J. Appl. Mech.

33. Greensmith, H. W., J. Pol. Sci., Vol. 21, (1956), pp. 175-187.

34. Greensmith, H. W., J. Appl. Pol. Sci. Vol. 3, (1960) pp. 175-182.

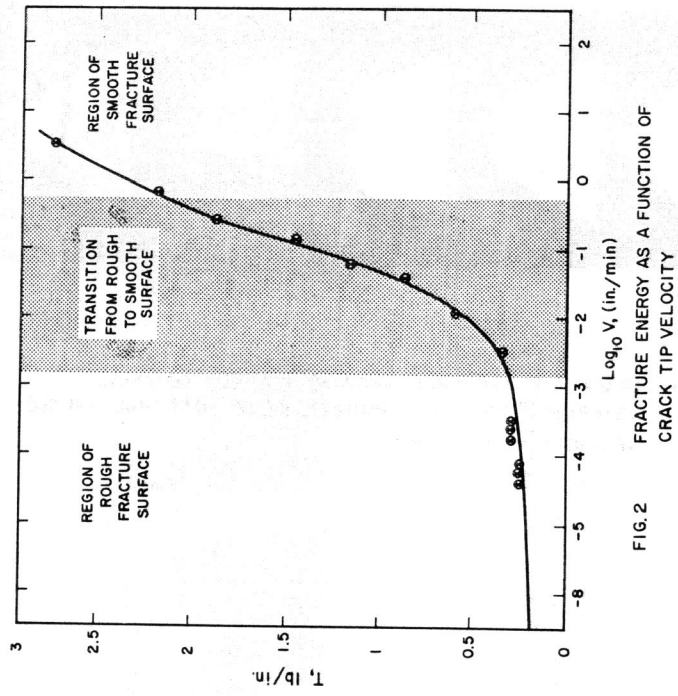

FIG. 2 FRACTURE ENERGY AS A FUNCTION OF CRACK TIP VELOCITY

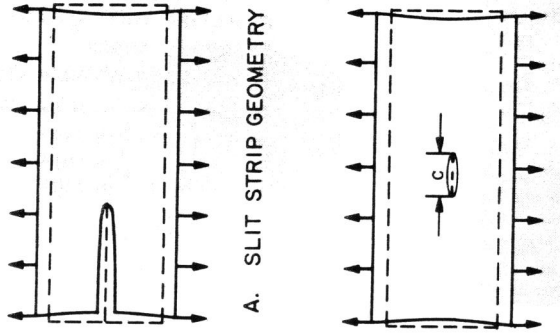

A. SLIT STRIP GEOMETRY

B. CRACKED STRIP GEOMETRY

FIG. 1 SHEET GEOMETRIES FOR CRACK PROPAGATION STUDIES

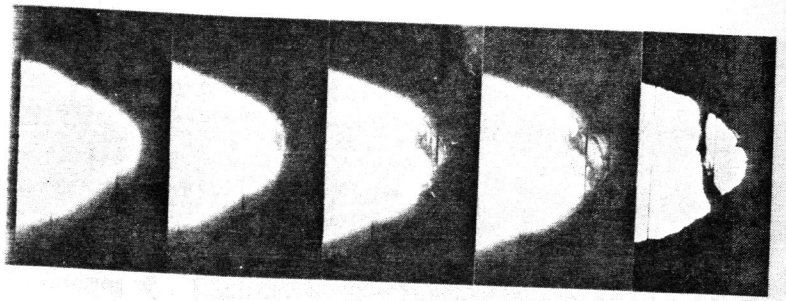

4X

FIG. 3 CRACK TIP SEQUENCE SHOWING FIBROUS MATERIAL DETERIORATION IN H-C RUBBER. (TIME INTERVAL ~ 15 SEC, VELOCITY ~ 0.1 IN./MIN.)

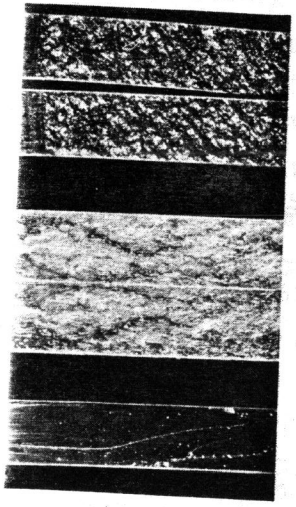

FIG. 4 FRACTURE SURFACES RESULTING FROM VARIOUS SPEEDS OF CRACK PROPAGATION. APPROXIMATE SPEEDS ARE, FROM TOP TO BOTTOM 10^{-3} IN./MIN.
1 IN./MIN.
10^{3} IN./MIN.

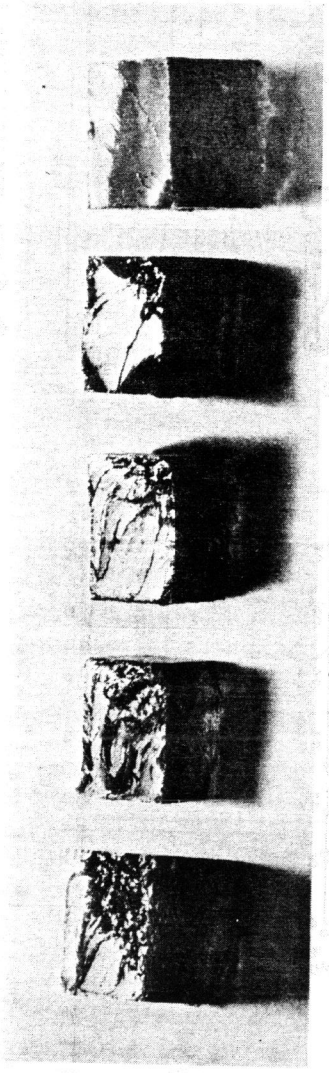

FIG. 5 APPEARANCE OF FRACTURE SURFACES OF SPECIMEN FAILED UNDER STRAIN RATES BETWEEN 10^{-3} AND 10^{3} IN./IN./MIN.. STRAIN RATE INCREASES FROM LEFT TO RIGHT.

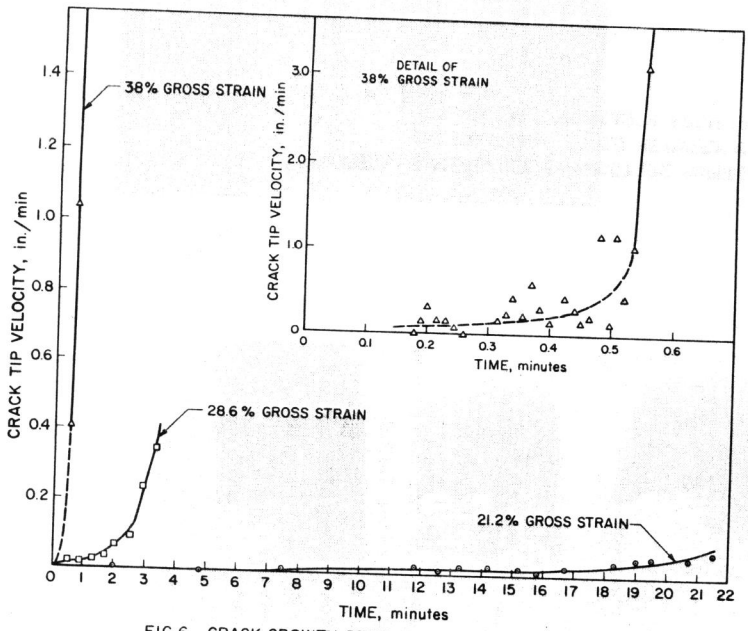

FIG. 6 CRACK GROWTH BEHAVIOR AS A FUNCTION OF TIME

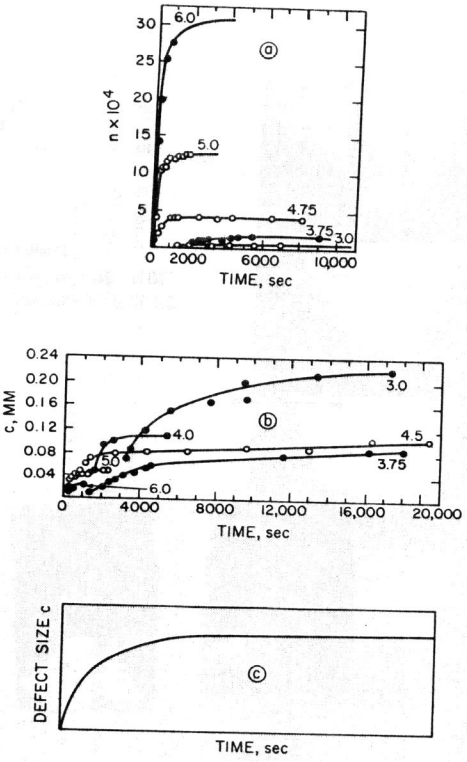

FIG. 7 QUALITATIVE COMPARISON OF DEFECT GROWTH

ⓐ and ⓑ DATA FROM REGEL'S PAPER, REF 24.
ⓐ NUMBER OF CRACKS n PER cm^2 OF THE SURFACE.
ⓑ CRACK LENGTH c
THE TENSION (in kg/mm^2) IS GIVEN NEAR EACH CURVE IN THE FIGURE.
ⓒ QUALITATIVE BEHAVIOR OF EQUATION 81.

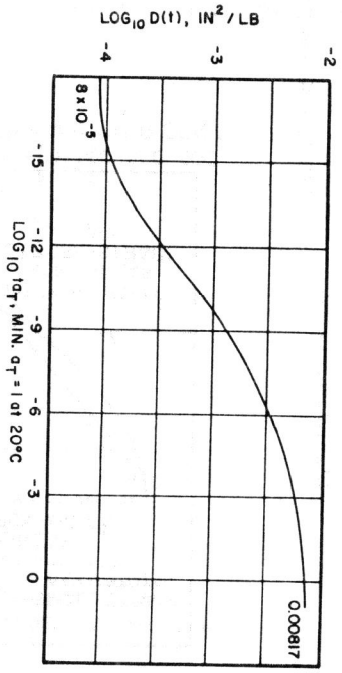

B. CREEP COMPLIANCE $D_{crp}(t)$ AS A FUNCTION OF TIME

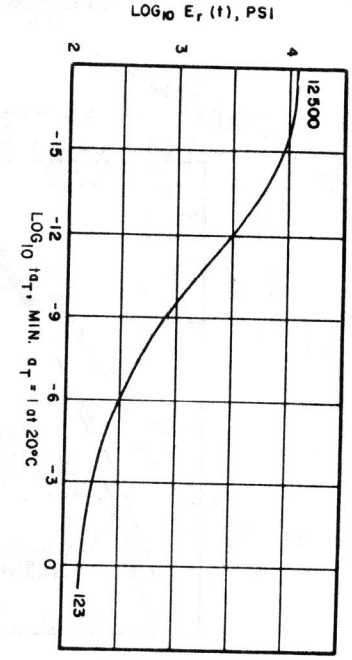

A. RELAXATION MODULUS $E_r(t)$ AS A FUNCTION OF TIME

FIG. 8 MECHANICAL PROPERTIES OF H-C RUBBER; TEMPERATURE = 20°C

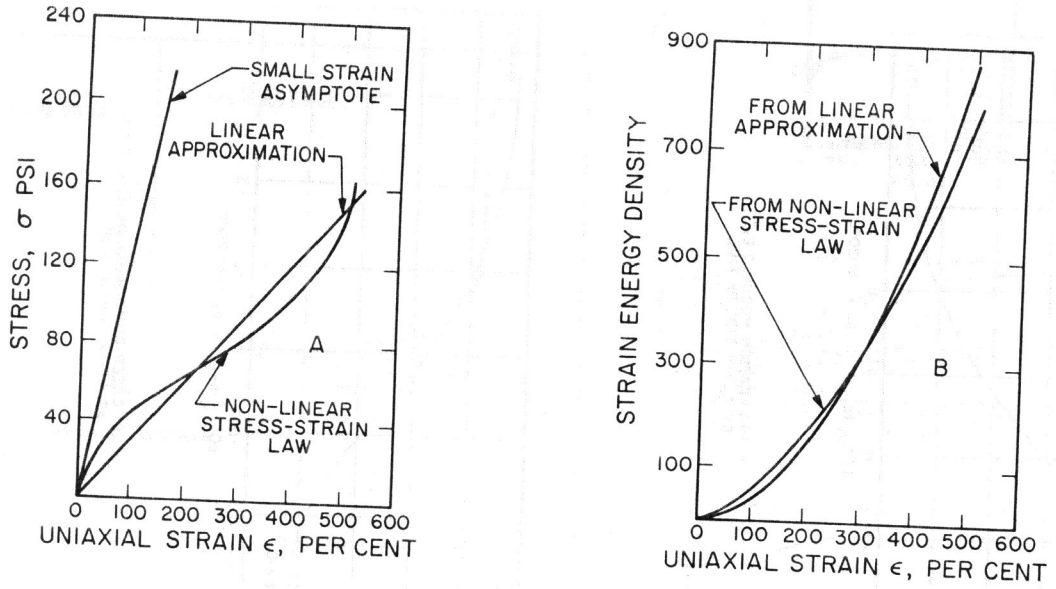

FIG. 9. COMPARISON OF STRESS, A, AND ENERGY DEPENDENCE, B, ON STRAIN FOR NON-LINEAR AND LINEARLY APPROXIMATED STRESS-STRAIN LAW

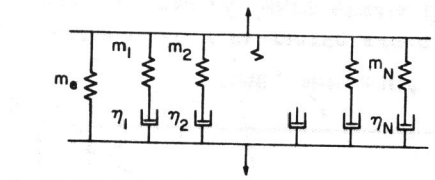

A. GENERALIZED MAXWELL OR WIECHERT MODEL

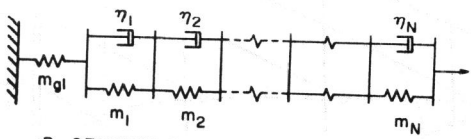

B. GENERALIZED VOIGT OR KELVIN MODEL

FIG. 10 MECHANICAL MODELS FOR A VISCOELASTIC MATERIAL

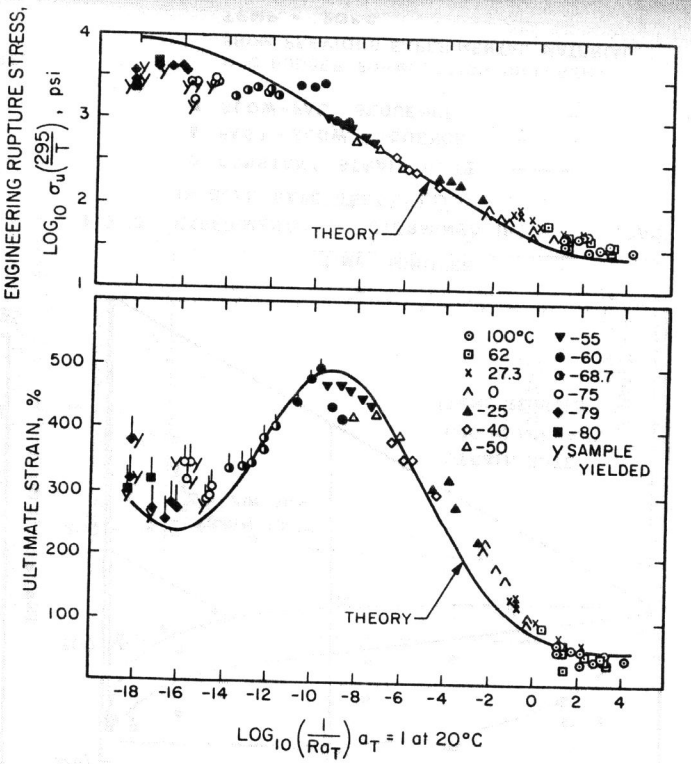

FIG. 11 ULTIMATE STRESS AND STRAIN IN AN ISOTHERMAL, UNIAXIAL CONSTANT STRAIN RATE TEST AS A FUNCTION OF TEMPERATURE REDUCED STRAIN RATE

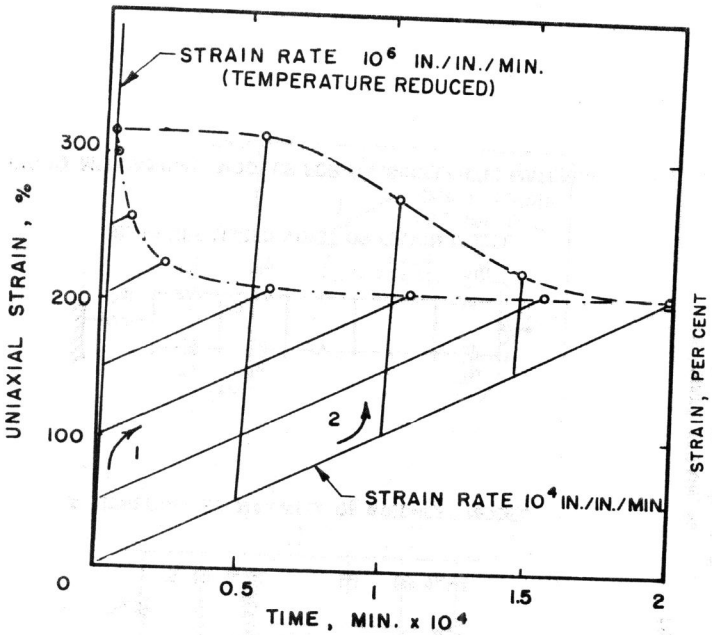

FIG. 12 THEORETICALLY PREDICTED EFFECT OF LOADING HISTORY UPON ULTIMATE STRAIN IN A DUAL STRAIN RATE TEST.

LINES DENOTE VARIOUS TRACES OF STRAIN. EXAMPLE; ARROW ① INDICATES SEQUENCE OF HIGH STRAIN RATE TO STRAIN OF 100 %, THEN LOW STRAIN RATE TO RUPTURE. ARROW ② INDICATES REVERSED SEQUENCE. CIRCLES DENOTE CALCULATED RUPTURE POINTS.

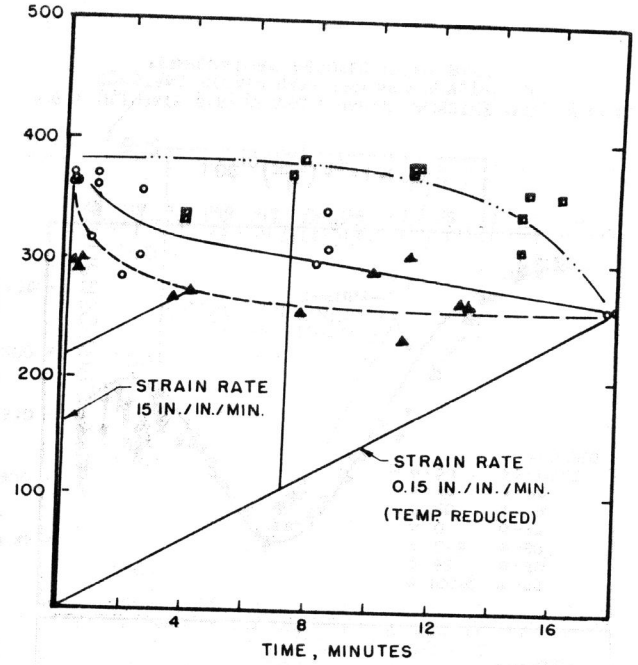

FIG. 13 EXPERIMENTALLY DETERMINED ULTIMATE STRAIN IN DUAL RATE TEST

- o CONSTANT STRAIN RATE ——
- ▲ FAST - SLOW SEQUENCE – – – –
- ▣ SLOW - FAST SEQUENCE —·—·—

H-G RUBBER FORMULATION DIFFERENT FROM PREVIOUS EXPERIMENTAL MATERIAL.
TEMP. = 20° C
(COURTESY K. HARSTAD, REF.)

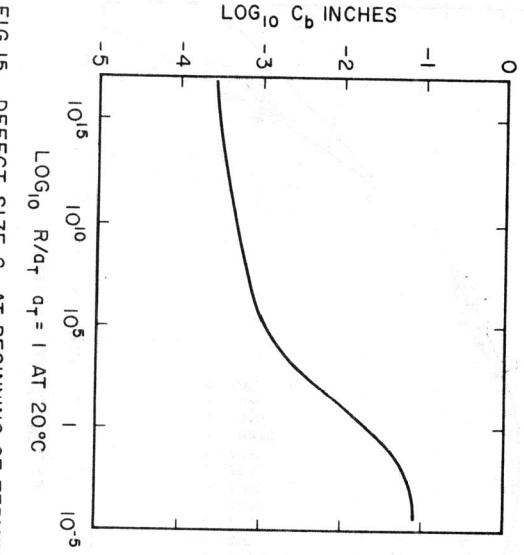

FIG. 15 DEFECT SIZE C_b AT BEGINNING OF TERMINAL CRACK PROPAGATION STAGE AS A FUNCTION OF TEMPERATURE REDUCED STRAIN RATE

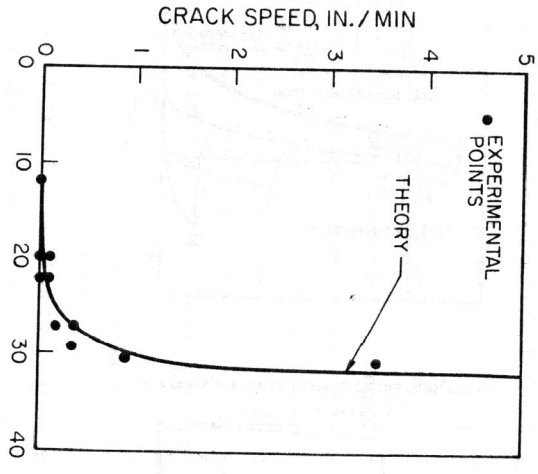

FIG. 14 CRACK PROPAGATION SPEED AS A FUNCTION OF GROSS STRESS IN STRIP SPECIMEN

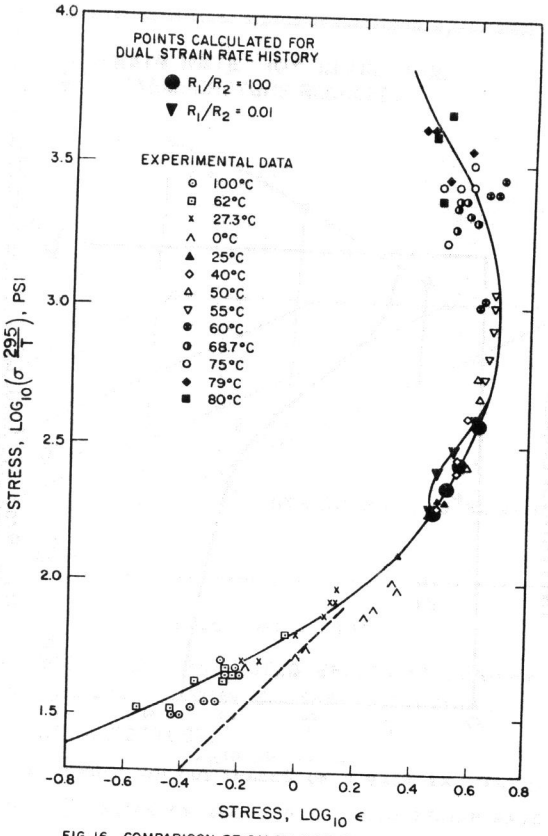

FIG. 16 COMPARISON OF CALCULATED FAILURE BEHAVIOR IN CONSTANT AND DUAL STRAIN RATE TEST WITH EXPERIMENTALLY DETERMINED FAILURE ENVELOPE.
DASHED CURVE IS BASED ON LINEARLY VISCOELASTIC STRESS STRAIN LAW, SOLID LINE CORRECTED FOR NON-LINEAR EFFECTS

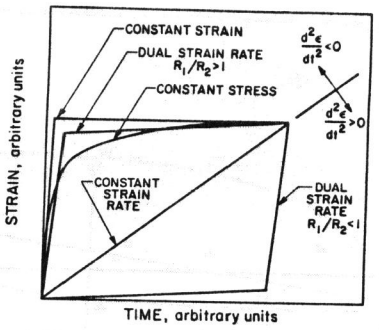

A. STRAIN HISTORIES LEADING TO THE SAME STRAIN

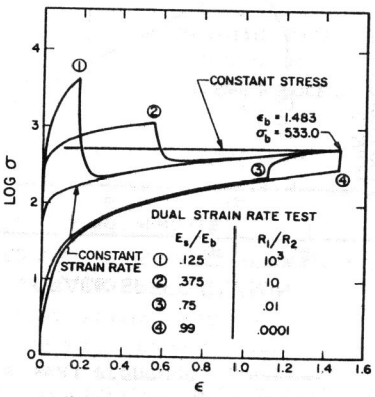

B. STRAIN HISTORIES LEADING TO THE SAME STRESS AND STRAIN ON THE FAILURE ENVELOPE

FIG. 17 SEVERAL STRAIN HISTORIES LEADING TO IDENTICAL VALUES OF STRESS AND STRAIN AT FAILURE (LINEARLY VISCOELASTIC BEHAVIOR OF A POLYURETHANE RUBBER)